Chemical Engineering Journal 181–182 (2012) 770–778

Contents lists available at SciVerse ScienceDirect

Chemical Engineering Journal

journal homepage: www.elsevier.com/locate/cej

Synthesis of exfoliated poly(styrene-co-methyl methacrylate)/montmorillonite nanocomposite using ultrasound assisted *in situ* emulsion copolymerization

B.A. Bhanvase[a], D.V. Pinjari[b], P.R. Gogate[b], S.H. Sonawane[a,c], A.B. Pandit[b,*]

[a] *Vishwakarma Institute of Technology, 666 Upper Indira Nagar, Pune-411 037, India*
[b] *Institute of Chemical Technology, N.P. Marg, Matunga, Mumbai-400 019, India*
[c] *University Department of Chemical Technology, North Maharashtra University, Jalgaon-425001, India*

ARTICLE INFO

Article history:
Received 14 June 2011
Received in revised form
15 November 2011
Accepted 22 November 2011

Keywords:
Ultrasound
P(MMA-*co*-St)/O-MMT composite
Emulsion copolymerization
Nanocomposites
Thermal stability

ABSTRACT

The present work deals with the synthesis of poly(methyl methacrylate-co-styrene)/montmorillonite [P(MMA-*co*-St)/O-MMT] nanocomposite using ultrasound assisted emulsion copolymerization operated in a semibatch manner. The synthesis process is based on dispersing montmorillonite (MMT) clay in the monomer (styrene) and surfactant (sodium dodecyl sulfate) under the influence of ultrasonic irradiations. Investigations have been carried out using treated MMT clay by quaternary ammonium salt (octadecylamine) as a starting material for establishing the dependency on the stability of emulsion and formation of latex. X-ray diffractrogram (XRD) have clearly established the complete exfoliation of MMT clay into the polymer. The exfoliated structure of nanocomposites has also been confirmed by transmission electron microscopy (TEM). It has been observed that both polymerization rate (R_P) and the fractional conversion decreased with an increase in the O-MMT clay loading in the emulsion polymerization system. The zeta potential and particle size analysis showed that nanocomposite latexes were electrostatically stable and average particle size was in the range of 156.58 to 191.23 nm with narrow particle size distribution. It has been observed that the exfoliated P(MMA-*co*-St)/O-MMT nanocomposite exhibits a higher glass transition temperature (T_g = 152.7 °C) and lower heat of reaction (ΔH = −265 J/g) at 1% O-MMT loading as compared to the neat copolymer (T_g = 127.3 °C, ΔH = −437.5 J/g). Nanocomposite formed using current method have been shown to give better thermal stability attributed to the interaction of O-MMT platelets with polymer leading to cross-linking enhancement.

1. Introduction

In the research area of material science, polymer/layered nanocomposite synthesis is one of the emerging areas due to the wide range of applications exhibited by the layered nanocomposites based on their versatile properties based on the combination of starting materials and the synthesis approach [1–6]. Two nanocomposites with dissimilar microstructures, namely exfoliated and intercalated could exist together when clay materials are dispersed into the polymer matrix [2]. In the intercalated composites, gallery spacing of layered silicate is increased by using a long chain organic molecule, which allows the occupation of the polymer chains into gallery spacing. In order to synthesize exfoliated nanocomposite structure, high mechanical shear is required to disperse the clay platelets into the host matrix [5]. Intercalated nanocomposite microstructure are suitable for development of barrier resistance nanocomposite application [4]. Exfoliated polymer clay hybrid structures offer superior mechanical and thermal properties, because of the homogeneous dispersion of clay in the polymer matrix, as well as a large interfacial area of clay layers interacting with the interspaced polymer layers [7].

Poly(methyl methacrylate) (PMMA) has excellent transparency and high modulus, but its melt viscosity is on a significantly higher side (>10^4 Pa s). It is also reported that mechanical properties of PMMA such as abrasion and wear are relatively low and independent of molecular weight. On the other side, polystyrene (PS) has relatively low modulus [8] and high abrasion resistance, load bearing capacity and greater tensile strength [9]. Thus the formation of a copolymer using these two polymers can compensate their demerits and the resulting composite material can have significant range of applications. The addition of clay to the polymer matrix can be further helpful in deciding the properties of the polymer matrix. Several methods such as melt mixing method [10], bulk polymerization [2,11–14], solution polymerization and emulsion polymerization [15–20] have been employed to synthesize copolymer/clay nanocomposite. Out of these techniques, emulsion polymerization has the important advantage of generating monodispersed polymer nanoparticles with controlled molecular

* Corresponding author. Tel.: +91 22 33612012; fax: +91 22 33611020.
E-mail address: ab.pandit@ictmumbai.edu.in (A.B. Pandit).

1385-8947/$ – see front matter © 2011 Elsevier B.V. All rights reserved.
doi:10.1016/j.cej.2011.11.084

weight and employment of water as a dispersion medium. Use of water results in possible widening of the galleries of layered silicates without any chemical treatment. Also encapsulation of materials is possible, if the inorganic particles are hydrophobic in nature [21]. Emulsion polymerization is an efficient technique for preparation of exfoliated structure of polymer/MMT composite. However, the level of shear in the reactor and the type of the clay modifier plays an important role in exfoliation of clay platelets in the organic phase [10,22]. Number of authors have reported the use of various surfactants to achieve the compatibility of clay and polymer matrix to yield better dispersion of the clay platelets in the polymer matrix [3,12,14,15]; however the effective dispersion of clay into the polymer matrix still remains a problem. Li et al. [15] have employed emulsion polymerization route for the synthesis of exfoliated PS/MMT nanocomposite using zwitterion as a clay modifier and observed that synthesized exfoliated PS/MMT nanocomposite shows an improvement in the storage modulus and glass transition temperature compared to the neat polystyrene and intercalated PS/MMT composites. Choi et al. [16] have used two stage emulsion polymerization, where delamination of clays into monomer emulsion was carried out in first stage followed by the polymerization to obtain core shell structure of poly(methyl methacrylate-*co*-styrene)/silicate nanocomposites in the second stage. Due to the successful delamination of clay into monomer during a first stage, an substantial improvement in the storage modulus (about 91%) has been observed. Xu et al. [19] used highly reactive, 2-acrylamido-2-methyl-1-propane sulfonic (AMPS) surfactant to widen the inter-gallery spacing of clay during styrene-co-methyl methacrylate emulsion polymerization. Diaconu et al. [20] have achieved high solid content of water-borne methyl methacrylate-co-butyl acrylate/clay nanocomposites by emulsion polymerization.

The passage of ultrasonic waves in the liquid medium is known to generate cavitation events where number of microbubbles are created which grow due to the pressure fluctuations and collapse adiabatically over a very small time scale [23]. The extreme adiabatic conditions generated locally are responsible for the generation of radicals by dissociation of the trapped organic/water molecules. Formation of intense turbulence coupled with strong liquid circulation currents can generate a very fine and stable emulsion [22] and also the dispersion or the mass transfer rates are significantly enhanced. Thus the use of ultrasonic irradiation as a intensified source of energy dissipation during the synthesis of polymer/clay nanocomposites is expected to yield beneficial results due to two simultaneous effects viz. shearing action generated by ultrasonic cavitation helps in exfoliation and homogeneous dispersion of clay into the organic phase [10,22] and secondly uniform size of monomer droplet can be achieved without any possibility of aggregation [24]. Cavitation has been also reported to help in the separation of silicate layers into the number of exfoliated platelets due to microstreaming phenomena [22]. The majority of the reports dealing with use of high intensity cavitation in polymer chemistry are based on the initiation of the polymerization reactions [24–26]. Few reports have been also found on the application of ultrasound during the initial stages of nanocomposite formation and melt mixing process. Ryu et al. [10] and Ryu and Lee [27] have synthesized poly(methyl methacrylate)–MMT nanocomposites using ultrasonic irradiations with an objective of dispersion of the clay platelets into the polymer melt during the melt mixing process. Borthakur et al. [22] studied the formation of core and shell poly(styrene-co-methyl acrylate)–bentonite nanocomposite using miniemulsion process and reported the application of ultrasound only in the stage one, i.e. during emulsion formation. It has been reported that the reduction of the particle size can be achieved till 700 nm, whereas some of the other reports with continuous use of ultrasound irradiation have shown a reduction in the particle size to less than 100 nm [24]. Continuous use of cavitation may facilitate the encapsulation, dispersion and/or segregation of the nanoparticles. It is also known that the Oswald ripening process can be eliminated or reduced. The observed elimination of the ripening has been attributed to the fact that shrinkage of monomer droplets (consisting of the inorganic core) is opposed by an increase of osmotic pressure (increasing free energy) of the trapped inorganic core. Further, continuous ultrasonic irradiation can also be used for generation of efficiently stabilized emulsion by incorporating inorganic core in monomer droplet and there exists a possibility that the requirement of the co-surfactant to reduce the Oswald ripening process can be eliminated [28,29].

Wang et al. [30] used ultrasound assisted emulsion polymerization for one-pot synthesis of montmorillonite–exfoliated polystyrene nanocomposite. Interestingly, it has been observed that the nanocomposite grew in one direction to form a bundle during the ultrasonic irradiation. This reported investigation indicated the noncontact directional control of certain materials by ultrasound. It has also been reported that ultrasonic irradiation successfully generates exfoliated nanocomposite with sufficient interaction between monomer and organic chains of the interlayer. Also, the clay aggregates in the ultrasonically processed nanocomposites are more finely dispersed than in the case of simple mixing methods [10,27]. Ultrasonic irradiations have also been used for emulsification (stage one) during the formation of core and shell poly(styrene-co-methyl acrylate)–bentonite nanocomposite using miniemulsion process [22]. Further, Wang et al. [31] have used high intensity ultrasound for the synthesis of intercalated polystyrene/Na^+-MMT nanocomposites by intercalating hydrophobic polystyrene into the hydrophilic silicate layers via ultrasonically initiated in situ emulsion polymerization. It has been reported that use of ultrasonic irradiations initiates polymerization reaction of monomer without any additional chemical initiator and also the silicates can be used without any modification. Enhanced breakup of layered silicate bundle and reduction in the size of dispersed phase with better homogeneity can be achieved by power ultrasound assisted in situ emulsion polymerization as compared to the conventional in situ emulsion polymerization. The shearing action generated by ultrasonic cavitation can be used for synthesis of exfoliated polymer/clay nanocomposite with homogeneous dispersion of clay into the organic phase. Furthermore, ultrasonic irradiation can not only initiate polymerization at room temperature and disperse clay layers at the nanoscale, but can also shorten the polymerization time. Therefore, the ultrasonically initiated in situ emulsion polymerization can be considered as a novel, simple, and fast approach to prepare polymer/layered inorganic nanocomposites. In the present work, an attempt was made to synthesize exfoliated structure of P(MMA-*co*-St)/O-MMT nanocomposite by ultrasound assisted semibatch emulsion copolymerization in the presence of modified MMT clay. To the best of our knowledge, there has been no previous study depicting the continuous use of power ultrasound during the formation of exfoliated structure of poly(methyl methacrylate-co-styrene)/O-MMT by semibatch in situ emulsion copolymerization. The ultrasonic irradiation has been achieved using direct probe type sonicator as it is expected that the high levels of shear help in the separation of a layered silicate bunch (tactoids) in the initial stage. The present work has clearly established the role of ultrasonic irradiations for an effective dispersion of clay into the polymer matrix based on the intensified shear and turbulence levels in the reactor.

2. Experimental

2.1. Materials

Methyl methacrylate (MMA, density: 0.936 g/cm^3 A.R. grade) and styrene (>99% purity) were procured from Sigma–Aldrich

and washed by using aqueous 0.1 N NaOH and demineralized water to remove the possible inhibitors present in the material. Analytical grade surfactant, sodium dodecyl sulfate (SDS, $NaC_{12}H_{25}SO_4$) and initiator potassium persulfate (KPS, $K_2S_2O_8$) were procured from S.D. Fine Chem., Mumbai and used as received from the supplier. Pristine sodium montmorillonite (MMT) with cation exchange capacity (CEC) of 119 meq/100 g clay (specific surface area, 274 m^2/g) was purchased from Sigma–Aldrich, USA. MMT was modified by using octadecylamine (mol. wt. 269.52, $CH_3(CH_2)_{17}NH_2$, stearylamine, organic modifier), which was procured from Aldrich and used as received. Demineralized water was used throughout the experimentation.

2.2. Intercalation of MMT by octadecylamine

Separation of impurities from natural MMT is necessary before the modification of clay and its subsequent use in the polymerization. This is attributed to the fact that the impurities may disturb the final properties of formed composite. With this background, the purification of available MMT has been carried out following the steps outlined below:

(1) Initially pristine clay was washed 3–4 times using demineralized water followed by centrifugation. Impurities such as silica and iron oxides were removed by differential sedimentation technique.
(2) Aqueous solution of MMT was stirred for 1 h and then kept undisturbed overnight. After subjecting the solution to centrifugation, the obtained solid was exposed to slow evaporation, until the desired dryness was obtained by keeping it at a temperature of 50 °C.

Octadecylamine has been used as a modifier to widen the gallery spacing between the platelets [32]. Modification of MMT was carried out by a cation exchange reaction. 11.9 g of octadecylamine (calculated based on CEC of MMT used) was dissolved in 250 ml of demineralized water containing 1.2 ml of hydrochloric acid (1 N) and the temperature of solution was maintained at 70 °C. 10 g of MMT was dispersed in 1000 ml water at 80 °C and was subsequently mixed with the octadecylamine solution prepared earlier. The resulting solution was stirred vigorously for 12 h followed by filtration to remove the precipitate. The obtained precipitate was washed with hot water for 1 h and centrifuged. The procedure was repeated several times such that all the unreacted amines were removed. The final precipitate was thoroughly dried in an oven at 80 °C for 24 h to obtain the modified MMT nanoclay (O-MMT).

2.3. Synthesis of P(MMA-co-St)/O-MMT nanocomposite by ultrasound assisted semi-batch in situ emulsion polymerization

P(MMA-co-St)/O-MMT nanocomposite synthesis was carried out in the emulsion polymerization reactor as shown in Fig. 1 and operated in semi batch mode. The experimental setup consists of a reactor which is basically a jacketed glass vessel of 500 ml volume capacity equipped with a 13 mm stainless steel probe connected to an ultrasonic generator (Sonics Vibra-cell, USA). The ultrasonic horn operates at a frequency of 22 kHz and the rated output power was 750 W. In the experiment, the ultrasonic horn is operated at 50% amplitude, meaning that the supplied power to the system was 375 W. The actual power dissipation by the probe sonicator was measured using a calorimetric method and it has been observed that the actual power dissipation is 46.4 W giving an energy transfer efficiency of 12.4%. All the experiments were carried out in the presence of nitrogen atmosphere to avoid contact of the reaction mass with the external oxygen.

In a typical run, the surfactant solution was prepared initially by adding 1.08 g of SDS in 100 ml of distilled water and was transferred to the ultrasound probe reactor. 11.9 ml of styrene was added to the ultrasound probe reactor along with O-MMT (0.5–5 wt % of the monomer quantity) and irradiated for 15 min using ultrasound to exfoliate nanoclay into the organic phase droplets. Reaction mixture was heated after addition of styrene, and the temperature was maintained at 60 °C (±1) throughout the duration of the experiment. In a separate beaker, initiator solution was prepared by dissolving 0.86 g of KPS in 20 ml water and then added dropwise into the reactor. Subsequently, MMA (total quantity of 11.5 ml) addition was carried out within first 30 min out of the total ultrasound irradiation reaction time of 1 h into the system at a rate of 0.38 ml/min. The complete reaction was carried over a period of 60 min in the presence of the ultrasonic irradiation to ensure complete exfoliation of the O-MMT clay in the polymer latex. Samples were withdrawn at regular intervals to monitor the percentage conversion by gravimetric analysis. These samples were dried in an oven at 150 °C until constant weight is obtained so that all the water and unreacted monomer are removed.

2.4. Characterization

The size and morphology of the nanoparticles of MMT embedded into the polymer matrix were determined by using a transmission electron microscope (TEM, model CM10, Philips). The structural properties of pristine MMT, O-MMT, P(MMA-co-St) have been studied by low angle X-ray diffraction (XRD) measurements using the CuKα radiation with λ = 1.5405 Å. An infrared (IR) spectrum of samples was also obtained using a Shimadzu 8400S FTIR spectrometer in KBr medium at room temperature in the region of 4000–500 cm^{-1}. Zeta-potential and *Z*-average diameter of neat P(MMA-co-St) copolymer and P(MMA-co-St)/O-MMT nanocomposite were determined on a Malvern Zetasizer (DTS Ver. 5.10) instrument. Monomer conversion was determined by gravimetric method during the semi-batch emulsion polymerization. The weight loss of sample was determined by using a thermogravimetric analysis (PerkinElmer TGA system, USA), from room temperature to 800 °C in N_2 atmosphere at a heating rate of 10 °C/min. The glass transition temperature (T_g) was measured by differential scanning calorimetry (Shimadzu DSC-60) in nitrogen atmosphere at a heating/cooling rate of 10 °C/min. Pencil hardness of the coatings was determined using standard pencils. Viscosity of the latex dispersion has been recorded using Haake Viscometer 550.

3. Results and discussion

3.1. Mechanism of exfoliated P(MMA-co-St)/O-MMT nanocomposite formation

An electrostatic attraction between the negatively charged ions present on an octahedral sheet of silicate layers and cations (Ca^{2+}, Na^+) present in the gallery results in a decrease in the gallery spacing. This reduction in gallery spacing hinders the intercalation of the long chain molecules and hence there is a need of additional agent such as surfactant to increase the *d*-spacing and hence the cation exchange capacity of clay [15]. In this work, octadecylamine is used as an intercalating agent, which contains an amino group ($—NH_2$) attached to a long chain carbon backbone (C18). Dilute aqueous HCl medium was used to protonize $—NH_2$ to formulate cationic $—NH_3^+$ in order to accomplish ion exchange with interlayer cations.

The mechanism of synthesis of exfoliated P(MMA-co-St)/O-MMT nanocomposite has been depicted in Fig. 2. In the first stage,

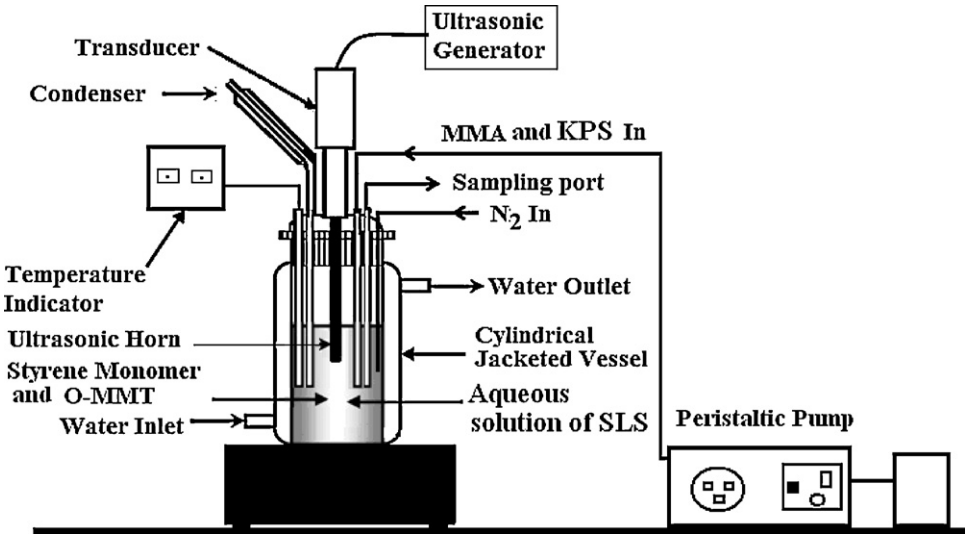

Fig. 1. Experimental setup for ultrasound assisted P(MMA-*co*-St)/O-MMT nanocomposite synthesis.

O-MMT is mixed with styrene in the presence of ultrasonic irradiations which help in obtaining the exfoliated structure. High shear levels associated with intense turbulence due to the cavitational effects result in clay exfoliation into single platelets, which can be then easily dispersed into the monomer phase [22]. The effective mixing of clay with monomer results into stable emulsion without phase separation [33]. In the second stage, OH group of SDS adsorbs at the edges of the O-MMT clay platelets. The polar carboxyl groups of the methyl acrylate and styrene interact with the polar groups (—OH) present on clay platelets [22,34]. The interaction between the polar groups leads to a formation of stable emulsion droplets of monomers containing platelets by reducing or elimination of Oswald ripening process [29]. During polymerization, radicals are generated in the aqueous phase by two mechanisms viz. by dissociation of initiator at higher temperature and by adiabatic implosion of cavities due to the ultrasonic irradiations [35]. It is also possible that the primary radicals generated by dissociation within the cavitating bubbles further react with the monomer molecules at the cavitation bubble/solution interface and generate additional radicals. The generation of enhanced quantum of radicals along with the reduced diffusion resistance due to turbulent conditions generated due to cavitational effects results in initiation and faster progress of the polymerization reaction [24,36]. The reduction in diffusion resistance occurs due to acoustic cavitation, which enhances the micro-vortex motion of ingredients leading to stirring effects in the reaction medium. Further, the polymerization of MMA with a styrene monomer takes place around the O-MMT clay platelets. This mechanism may contribute to the exfoliation

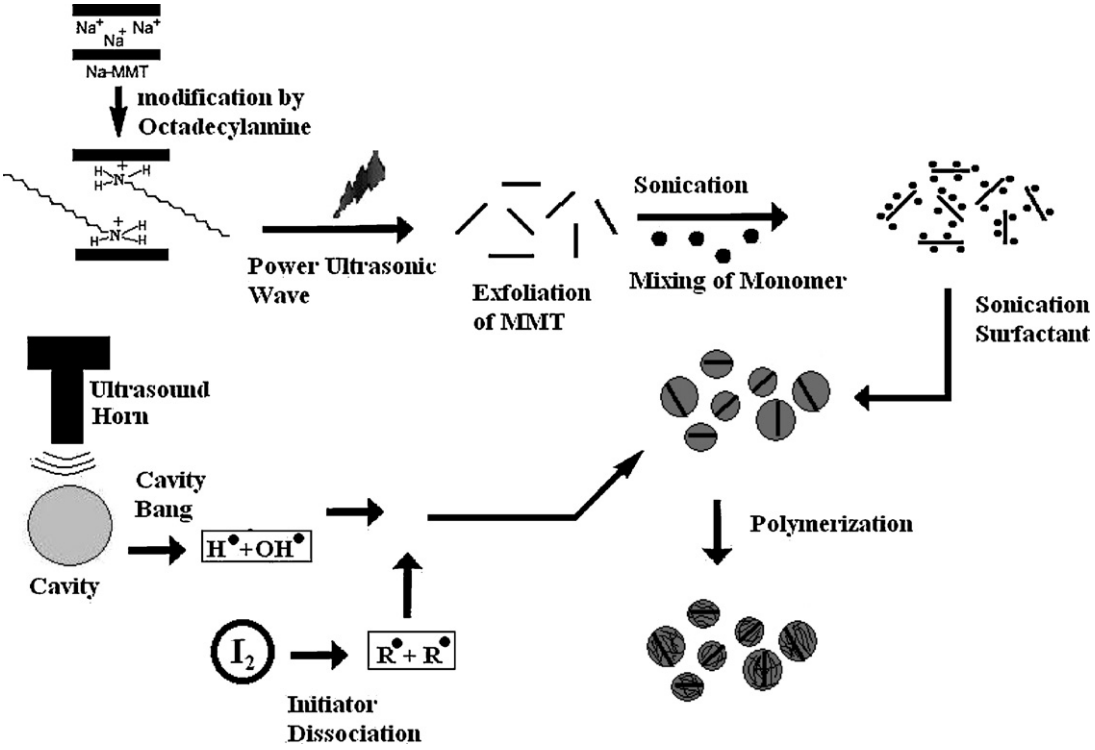

Fig. 2. Schematic mechanism for exfoliation of MMT and the formation process of P(MMA-*co*-St)/O-MMT nanocomposite.

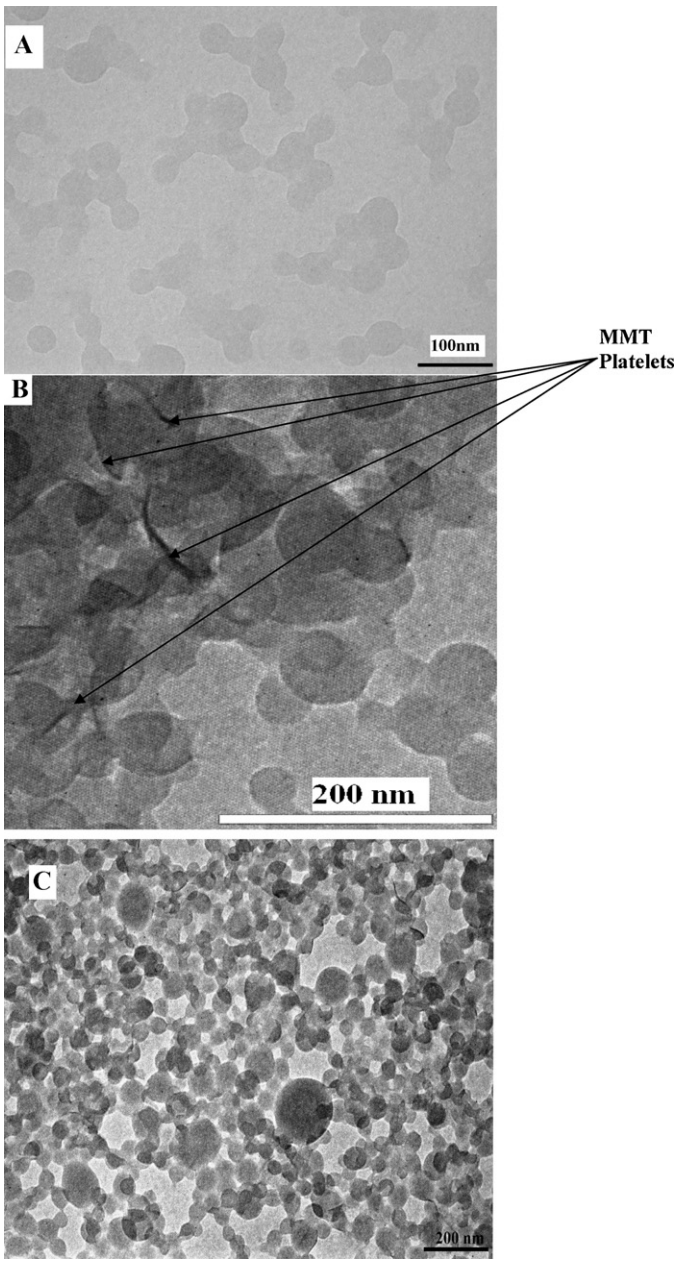

Fig. 3. TEM image of (A) P(MMA-*co*-St) nanoparticles; (B) and (C) P(MMA-*co*-St)/O-MMT nanocomposite with 4% loading of O-MMT clay.

of nanocomposites leading to exfoliated structure of the P(MMA-co-St)/O-MMT nanocomposite. Fig. 3A–C shows the TEM images of P(MMA-co-St) and P(MMA-co-St)/O-MMT nanocomposite. It has been clearly observed that the O-MMT layers are finely dispersed in the P(MMA-co-St) latex giving rise to exfoliated structure of P(MMA-co-St)/O-MMT nanocomposite. TEM image of P(MMA-co-St) (Fig. 3A) shows that the polymer particles are spherical in nature with size around 50 nm. In contrast, P(MMA-co-St)/O-MMT nanocomposite images show the presence of MMT platelets dispersed in these polymer latex. P(MMA-co-St)/O-MMT nanocomposite shows the particle size to be less than 100 nm, which is substantially lower as compared to the nanocomposite synthesized using conventional in situ emulsion polymerization. The observed decrease in the size of the nanocomposite can be attributed to the reduction in initial monomer droplet size obtained by ultrasonic irradiation, and improvement in the dispersion of clay platelets in the polymer matrix due to the continuous ultrasonic irradiation.

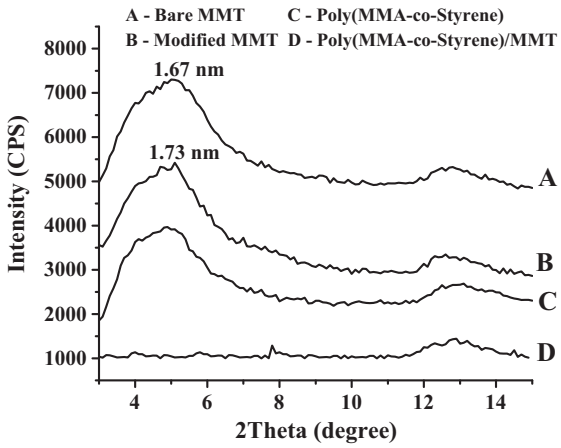

Fig. 4. XRD pattern of (A) pristine MMT, (B) modified MMT, (C) P(MMA-*co*-St) nanoparticles, and (D) P(MMA-*co*-St)/O-MMT nanocomposite with 4% loading of O-MMT clay.

3.2. XRD analysis of P(MMA-co-St)/O-MMT nanocomposite

Fig. 4 shows the XRD patterns of the pristine MMT, O-MMT, P(MMA-co-St) and P(MMA-co-St)/O-MMT nanocomposite. The pristine MMT (Fig. 4 pattern A) shows an interlayer spacing of $d = 1.67$ nm at 2θ value of 5.3°, which is calculated by using Bragg's equation: $2d \sin\theta = \lambda$ where d is the interplanar distance, θ is the diffraction angle and λ is the wavelength. Fig. 4 pattern B depicts the X-ray diffraction pattern of O-MMT. Prominent peak at 5.1° corresponds to the basal space of 1.73 nm, which indicates that the interlayer spacing of silicate is improved due to the presence of octadecylamine. Fig. 4 pattern C shows the XRD pattern of P(MMA-co-St). Broad peak around 5° is observed which indicates that the copolymer material is mainly amorphous.

In the case of P(MMA-co-St)/O-MMT, (Fig. 4 pattern D) the prominent peak at 5.1° is departed, which signifies the complete exfoliation of clay [37]. The complete exfoliation is possible because of the high shear effect of ultrasonic irradiation during emulsion polymerization [10,22]. The platelets can be exfoliated in the polymer matrix due to a large spacing between the layers and cavitational jet effect. Complete de-lamination of individual clay platelets into the entire matrix of P(MMA-co-St) occurs which also indicates a 'polarity match' with the clay surface and results into favourable interaction of clay and polymer, hence peak observed at the 5° in XRD pattern of P(MMA-co-St) disappears in the case of P(MMA-co-St)/MMT nanocomposite. Thus, the XRD analysis has confirmed that the use of hydrophobic modifier, surfactant and ultrasonic irradiations helps to obtain an exfoliated structure of P(MMA-co-St)/O-MMT nanocomposite.

3.3. FTIR analysis of P(MMA-co-St)/O-MMT nanocomposite

Fig. 5 shows an infrared spectra of the MMT, O-MMT, P(MMA-co-St) and P(MMA-co-St)/O-MMT nanocomposite in the range of 4000–400 cm^{-1}. As shown in Fig. 5 (pattern A), transmittance peaks of pristine MMT shows —OH stretching of silicate layers at 3647 and bending of the OH groups at 1651 cm^{-1}, while Si—O stretching is observed at 1111 cm^{-1}. Si—O—Al bending vibrations are found in the range of 400–600 cm^{-1}. Fig. 5 (pattern B) shows an infrared spectra of octadecylamine modified MMT. Peaks at 1467 and 2851 cm^{-1} represents the stretching vibrations of an alkyl group ($—CH_3$). NH bending was found at 1499 cm^{-1} and the obtained peak at 2920 cm^{-1} shows the presence of a halo-alkyl group ($CH_3—Cl$) due to the addition of octadecylamine. Peaks of silicon based esters such as R—O—Si—O— noticed in the range of

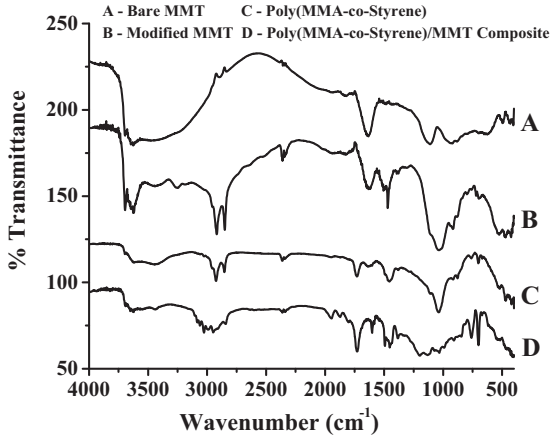

Fig. 5. FTIR spectra showing various bonds in (A) pristine MMT; (B) modified MMT; (C) P(MMA-*co*-St) nanoparticles; (D) P(MMA-*co*-St)/O-MMT nanocomposite with 4% loading of O-MMT clay.

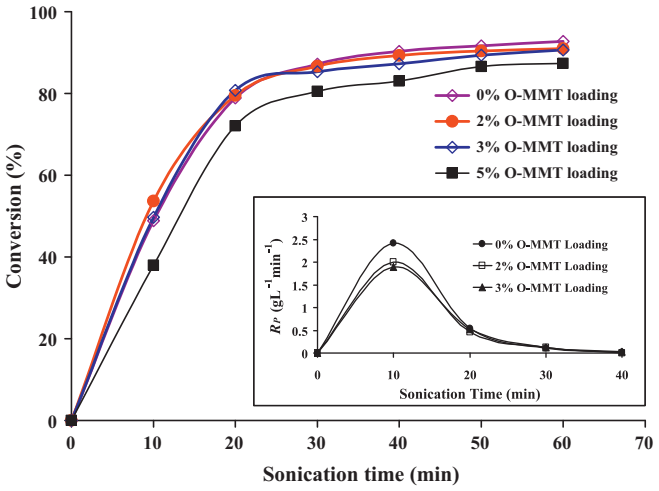

Fig. 6. Conversion as a function of time at different percentage of O-MMT clay loading (Inset: polymerization rate (R_P) vs sonication time).

400–797 cm^{-1} are attributed to the presence of aluminosilicates. Transmittance peaks at 2924, 2854 cm^{-1} observed in Fig. 5 (pattern C) represents the C—H stretching, while the peaks at 1730 represent C=O stretching. Further peaks at 1000–1200 cm^{-1} represent C—O stretching. The characteristic peaks at 760 cm^{-1} represent the aromatic C—H bending due to PMMA-co-St polymer. As shown in Fig. 5 (Pattern D) characteristic peaks at 3647, 1604 (—OH bending of silicate layers), 1033 (Si—O stretching) and 400–600 cm^{-1} (Si—O—Al bending vibration) clearly indicates the presence of O-MMT in the finally synthesized P(MMA-co-St)/O-MMT nanocomposite. The peak at 1651 cm^{-1} is attributed to the presence of the ester carbonyl (C—O) asymmetric functional group. This peak appears to be shifted to 1735 cm^{-1} in the pattern D due to the introduced modifications in MMT (O-MMT) clay. The transition of asymmetric C=O to the C—O—C symmetric vibrations in the presence of O-MMT confirms the interaction between the clay platelets of O-MMT and the polymer surface. Further, peak at 2920 cm^{-1} is attributed to the C—H stretching vibrations due to the CH_2 bands. In the case of composite, this peak is shifted to 3032 cm^{-1} indicating the presence of C—H stretching vibrations due to the CH_3 bands. This shifting of the MMT peak is also attributed to the interaction of the silicate layer of O-MMT clay with the polymer surface. Overall it can be said that the FTIR investigations have clearly established that the O-MMT has been successfully incorporated in the polymer matrix.

3.4. Styrene and MMA emulsion copolymerization kinetics in the absence and presence of O-MMT clay at different clay loading

The influence of O-MMT clay loading on the conversion has been depicted in Fig. 6. It has been observed that the final conversion of monomer is decreased when the O-MMT clay content was increased. The maximum conversion in the absence of clay reached approximately 92.7%, and decreased subsequently to 91, 90.6, and 87.3% when the clay content increased to 2.0, 3.0, and 5.0%, respectively. Fig. 6 also shows that the conversion of the pure monomer system reached the maximum value at the reaction time of 60 min and thereafter levelled off. The conversion values do not change after reaction times of 60 min at different O-MMT clay loading. Further, the polymerization rate dramatically increases at the beginning of a reaction (0–10 min) for all O-MMT loading cases. The polymerization rate reaches the maximum value (Fig. 6 inset) and then decreases for all the cases. It is different from a classical conventional emulsion polymerization where the maximum polymerization rate remains constant [38]. In classical conventional emulsion polymerization process polymerization rate trend can be roughly divided into three different intervals, namely Interval I (particle nucleation), II (monomer transferring), and III (particle growth). Ultrasonic irradiations are responsible to alter the rates, as cavitation jets facilitate the transport of generated free radicals very fast towards the monomer droplet which results into an initial increase in the rates reaching maxima. In this distinctive feature of emulsion polymerization, the droplet nucleation is the dominating initiation mechanism, which results in a continual decrease of the monomer concentration. This leads to the decrease in the polymerization rate after the initiation stage. It has been also observed that the rate of polymerization for pure monomer emulsion systems attains the maximum value and decreases with an increase in the O-MMT clay loading. This is due to a decrease in the reactivity of radicals and living polymers in the presence of clay particles as the adsorption of these species occurs on the large nanoclay surface. In general, this study clearly indicates that the nanoclay introduced in the system has a hindered effect on the polymerization rate and the fractional conversion.

In the current study, conversion of monomer at the end of 60 min is 92.7% with the use of ultrasonic irradiation, where as it has been reported that for high conversion time required in the case of classical conventional emulsion polymerization was around 4–5 h [18,19]. This clearly indicates that the ultrasound assisted emulsion polymerization takes place in lesser time compared to conventional emulsion polymerization with improved polymerization rate, narrow molecular weight distribution, particle size distribution and higher monomer conversion [24].

3.5. Particle size and zeta potential of P(MMA-co-St)/O-MMT nanocomposites

The average particle diameters of all nanocomposites were observed to be in the range of 156.58–191.23 nm (Table 1) exhibiting fine particle size and also the distribution showed only one narrow peak (Fig. 7). These results are very much comparable with the results obtained from the TEM analysis. The average particle size of the P(MMA-co-St)/O-MMT nanocomposite is significantly lower as compared to the nanocomposite synthesized using conventional in situ emulsion polymerization. This observed decrease in the average particle size of the nanocomposite is due to the reduction in initial monomer droplet size obtained by ultrasonic irradiation, in which effective dispersion of clay platelets is accomplished by continuous ultrasonic irradiation. The results clearly

Table 1
Effect of O-MMT loading on glass transition temperature, *Z*-average diameter, zeta potential values, pencil hardness and heat of reaction of the P(MMA-*co*-St)/O-MMT nanocomposite latexes. (Temperature = 60 °C, weight of monomer = 21.52 g, MMA:St ratio = 1:1, weight of KPS = 0.86 g, weight of SLS = 1.08 g, and weight of water = 120 g.)

Sr. no.	Sample	Wt. of O-MMT (g) (% of O-MMT loading)	Glass transition temperature (°C)	Heat of reaction (J/g)	Zeta potential (mV)	*Z*-average diameter (nm)	Pencil hardness
1	Neat P(MMA-*co*-St)	0.00 (0.0)	127.3	−437.5	−46.4	52.64	HB fail
2	P(MMA-*co*-St)–0.5% O-MMT	0.11 (0.5)	129.1	−292.5	−46.7	156.58	HB fail
3	P(MMA-*co*-St)–1% O-MMT	0.22 (1.0)	152.7	−265	−48.8	168.88	HB fail
4	P(MMA-*co*-St)–2% O-MMT	0.43 (2.0)	131.8	−350	−42.8	170.74	HB fail
5	P(MMA-*co*-St)–3% O-MMT	0.65 (3.0)	130.4	−458	−40.4	178.28	HB pass
6	P(MMA-*co*-St)–4% O-MMT	0.86 (4.0)	129.8	−448	−37.1	185.72	HB pass
7	P(MMA-*co*-St)–5% O-MMT	1.08 (5.0)	129.0	−382	−35.8	191.23	HB pass

indicate the utility of the approach based on continuous use of ultrasonic irradiations throughout the polymerization process.

In addition, zeta potential values which are indicative of the homogeneity and stability of polymer nanocomposite latexes have been observed to slightly increase at higher percentage of clay loading. The zeta potential value of the neat P(MMA-co-St) copolymer was −46.4 mV while the zeta potential values of the P(MMA-co-St)/O-MMT nanocomposites increased from −42.8 to −35.8 mV for 2–5% O-MMT loading (Table 1). It has been observed that most of the zeta potential values of P(MMA-co-St)/O-MMT nanocomposite are well below than that of neat P(MMA-co-St) copolymer latexes indicating an increased latex stabilities. It has been reported by Yilmaz et al. [39] that the layered silicates should result in a decrease in the latex stability. However, the self arrangement of the silicate layers within the polymer particles may influence the surface tension and thus the stabilization of the latexes. Further, use of ultrasonic irradiation during in situ emulsion polymerization may cause fine and stable emulsion, which leads to reduction in the size of polymer nanocomposite particle. Also, hydrophobicity of O-MMT ensures clay position in the monomer phase, which promotes exfoliation and the clay platelets could get encapsulated by the polymer particles. On these grounds the increase in particle size and/or decrease in zeta potential values of the polymer nanocomposite latex are possible.

3.6. Thermal analysis of P(MMA-co-St)/O-MMT nanocomposite

Thermo gravimetric analysis (TGA) and differential thermal analysis (DTA) has been used to compare the thermal stability of nanocomposite synthesized in the present work with the pristine copolymer. The TGA plots as obtained for the P(MMA-*co*-St) nanoparticles, P(MMA-*co*-St)–2% O-MMT and P(MMA-*co*-St)–5% O-MMT nanocomposite have been shown in Fig. 8A–C, respectively. It can be clearly seen from the TGA plots shown in Fig. 8 that the onset temperature at which 20% weight loss of the material occurs is slightly shifted in the case of P(MMA-co-St)/O-MMT nanocomposite as compared to the pristine copolymer, which can attributed to the addition of O-MMT in the nanocomposite. The onset degradation temperature at 20% weight loss was raised from 384.1 °C (pristine P(MMA-*co*-St)) to 384.5 and 385.4 °C for P(MMA-*co*-St)–2% O-MMT and P(MMA-*co*-St)–5% O-MMT nanocomposite, respectively [18]. However, after 50% weight loss the P(MMA-co-St)/O-MMT nanocomposite shows higher thermal stability as compared to the pristine copolymer. The onset degradation temperature at 60% weight loss is 410.5 °C for pristine P(MMA-*co*-St) whereas it is 413.9 and 415.5 °C for P(MMA-*co*-St)–2% O-MMT and P(MMA-*co*-St)–5% O-MMT nanocomposite, respectively. The hindrance in the diffusion of volatile products from the clay layer and interaction of O-MMT platelets with the polymer leads to the cross-linking reaction [40,41]. It is also observed that the weight loss of P(MMA-*co*-St) polymer latex, P(MMA-*co*-St)–2% O-MMT and P(MMA-*co*-St)–5% O-MMT nanocomposite at 445 °C is found to be 95, 92 and 91 wt.%, respectively. These two observations in terms of the onset temperature and the weight loss indicates that O-MMT improves the thermal stability of the P(MMA-co-St) matrix. It is also plausible that the exfoliated structure of the clay acts as a nucleating agent in the polymer by absorbing the heat (acting as a heat sink) and hence strengthens the nanocomposite structure by avoiding degradation.

The DTA plots of pure P(MMA-*co*-St), P(MMA-*co*-St)–2% O-MMT and P(MMA-*co*-St)–5% O-MMT nanocomposite have been given in Fig. 9. Similar to pristine P(MMA-*co*-St), the P(MMA-*co*-St)/O-MMT nanocomposite revealed two-stage endothermic degradation during the overall decomposition process. The initial decrement in the mass is observed at 50 °C, which represents the dehydration of hydrophilic pristine P(MMA-*co*-St) and P(MMA-*co*-St)/O-MMT nanocomposite. In the second stage, decrease in the mass is due to the degradation of P(MMA-*co*-St) polymer backbone. In this case, as

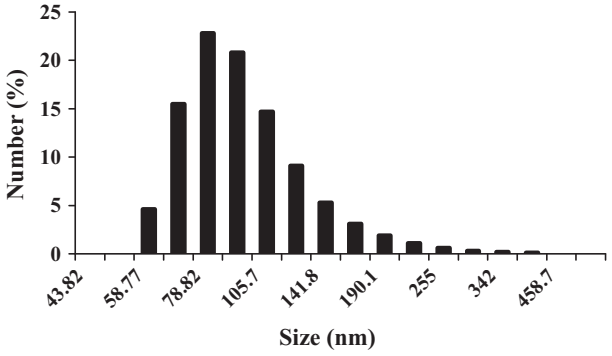

Fig. 7. Particle size distributions of the representative P(MMA-*co*-St)/O-MMT nanocomposite for 4% loading of O-MMT clay.

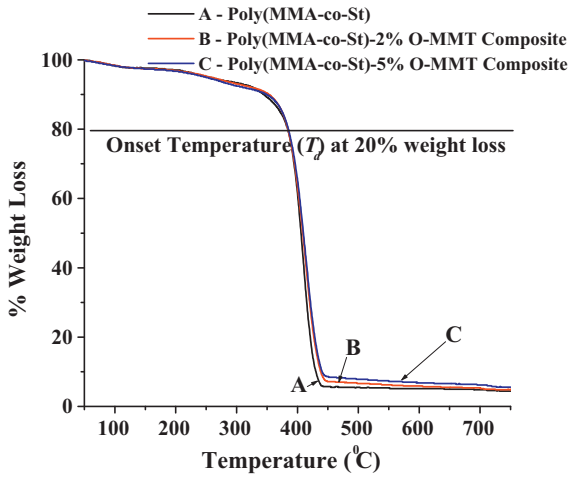

Fig. 8. Thermogravimetric analysis (TGA) plots of (A) P(MMA-*co*-St) nanoparticles; (B) P(MMA-*co*-St)–2% O-MMT nanocomposite and (C) P(MMA-*co*-St)–5% O-MMT nanocomposite.

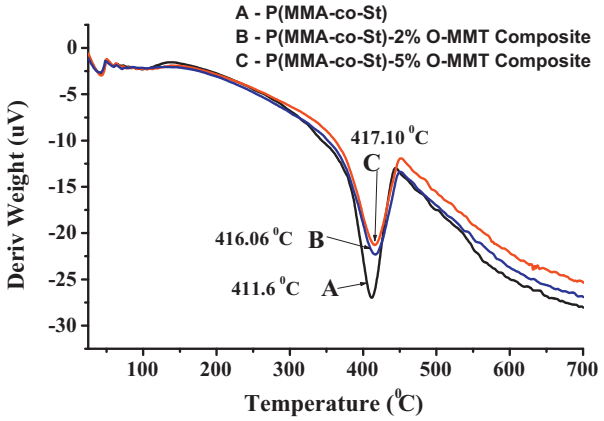

Fig. 9. DTA plots of (A) P(MMA-*co*-St) nanoparticles; (B) P(MMA-*co*-St)–2% O-MMT nanocomposite and (C) P(MMA-*co*-St)–5% O-MMT nanocomposite.

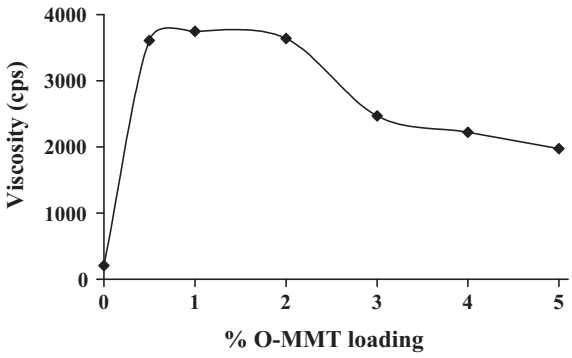

Fig. 10. The viscosity (cps) of latex dispersion at different clay loading.

compared to the pristine polymer, the difference in decomposition temperature of the P(MMA-*co*-St)–2% O-MMT and P(MMA-*co*-St)–5% O-MMT nanocomposite is marginal and it was 4.5 and 5.5 °C, respectively, which is higher in the presence of nitrogen atmosphere. The thermal behaviour of the P(MMA-*co*-St)/O-MMT nanocomposite in N_2 atmosphere indicates that the addition of O-MMT retards the thermal decomposition.

It has also been established by the differential scanning calorimetry (DSC) investigations that the presence of the O-MMT increases the glass transition temperature (T_g) of the P(MMA-*co*-St)/O-MMT nanocomposite. The obtained data have been given in Table 1. The obtained results confirm that the presence of O-MMT in nanocomposite restricts the motion of polymer segmental chains [42]. It is found that the glass transition temperature increases from 127.3 °C (pristine P(MMA-*co*-St)) to a maximum of 152.7 °C at 1% O-MMT loading. However, a further increase in the loading of O-MMT results in a decrease in the glass transition temperature as compared to optimum loading, though it is still higher as compared to the pristine P(MMA-*co*-St). The observed decrease in the glass transition temperature at higher loadings of O-MMT can be attributed to the agglomeration of polymer chains as there is a weak physical interaction between polymer chains and O-MMT. It has been also observed from the analysis that the value of ΔH (heat of reaction) for neat copolymer is higher as compared to nanocomposite for 1% O-MMT loading (−437.5 and −265 J/g for neat copolymer and nanocomposite, respectively). Reduction in ΔH indicates that the added O-MMT in the copolymer reduces exothermicity of the polymer matrix. The O-MMT platelets absorb the heat of reaction of copolymer leading to an increase in the overall crystallinity of the nanocomposite. Similar to the trends for glass transition temperature, the heat of reaction also decreases at higher loading of the O-MMT as compared to the optimum value of loading as 1%.

3.7. Mechanical properties (scratch resistance) of P(MMA-co-St)/O-MMT nanocomposite

Pencil hardness test is a simple and effective technique to evaluate the scratch resistance property of the coatings. Pencil hardness of P(MMA-*co*-St)/O-MMT nanocomposite has been compared with the pure P(MMA-*co*-St) polymer and respective values are enlisted in Table 1. It has been observed that the P(MMA-*co*-St)/O-MMT nanocomposite with 3% and higher O-MMT clay loading passes HB pencil hardness. Exfoliated nature of the nanocomposites may be the reason for increasing the surface hardness. However, pencil hardness for neat P(MMA-*co*-St) copolymer and P(MMA-*co*-St)/O-MMT nanocomposite for lower loading of O-MMT clay (0.5–2%) fails for HB. The pencil hardness of P(MMA-*co*-St)/O-MMT nanocomposite at higher loading of O-MMT is better compared to lesser loading of O-MMT because of well dispersion of O-MMT clay platelets (inorganic segments) into organic segments, i.e. P(MMA-*co*-St) polymer. Similar type of analysis is reported by Kuraoka and Ueno for clay/poly(methyl methacrylate) nanocomposites [43].

3.8. Rheological properties (viscosity) of P(MMA-co-St)/O-MMT nanocomposite

Viscosity of the P(MMA-*co*-St)/O-MMT nanocomposite latex dispersion at different O-MMT clay loading has been depicted in Fig. 10. It is well known that the addition of nanoclay will cause a significant increase in the monomer viscosity, even can form a gel at high concentration of nanoclay. The viscosity of the latex dispersion is increased with an increase in the O-MMT clay loading upto 2% loading beyond which a marginal decrease is observed. It may be attributed to aggregation of O-MMT in the polymer latex dispersion, which is consistent with the discussion reported in earlier sections. Further, because of the increase in the latex dispersion viscosity, the molecular diffusion of initiator, monomer and living polymer inside the monomer droplet/micelles containing O-MMT clay could be significantly reduced. Consequently, monomer conversion and polymerization rate is significantly decreased in presence of O-MMT clay which is in line with the discussion made in the earlier section where an effect of O-MMT loading on the polymerization rate and monomer conversion has been discussed. Furthermore, it has been noted that the particles size increases at high clay concentration with increased viscosity. The use of ultrasonic irradiation during in situ emulsion polymerization may cause fine and stable emulsion, which leads to reduction in the size of polymer nanocomposite particle compared with conventional in situ emulsion polymerization. It has been also established that because of ultrasonic irradiation the homogeneity and stability of polymer nanocomposite latexes increased with percentage of clay loading. Similar observation was drawn in the case of particle size and zeta potential analysis of P(MMA-*co*-St)/O-MMT nanocomposite.

4. Conclusions

The present work has established that the ultrasonic irradiations can be effectively used for the synthesis of the exfoliated structure P(MMA-*co*-St)/O-MMT nanocomposite using the emulsion copolymerization of methyl methacrylate with styrene. It has been also confirmed that the surfactant, octadecylamine, can be effectively used to increase the interlayer spacing (*d*-spacing) of MMT galleries due to the interactions with the clay cations. The complete exfoliation of the O-MMT particles within the polymer matrix has also been confirmed using the TEM analysis. The results of thermogravimetric analysis confirm that the nanocomposite is thermally

stable than the pristine polymer. The glass transition temperature increased from 127.3 °C (pure P(MMA-*co*-St)) to 152.7 °C (upto 1% O-MMT loading) due to fine dispersion of exfoliated O-MMT in polymer latex. Further, it can be concluded that the addition of O-MMT clay hinders the rate of polymerization and the final conversion of monomer during in situ semibatch emulsion polymerization. It has been also established that ultrasound assisted emulsion polymerization for the synthesis of the exfoliated structure P(MMA-*co*-St)/O-MMT nanocomposite requires lower time (1 h) with improved polymerization rate and the dispersion of MMT in polymer latex compared to the conventional emulsion polymerization method, which requires around 5 h. The average particle diameters of all nanocomposites were in the range from 156.58 to 191.23 nm exhibiting fine particle size and the narrow particle size distributions with only one peak. It has been observed that most of the zeta potential values of P(MMA-co-St)/O-MMT nanocomposite are well below than that of neat P(MMA-co-St) copolymer latexes indicating increased latex stabilities. Overall, the present work has shown an approach for effective synthesis of nanocomposites with higher thermal stability elucidating the critical roles played by the ultrasonic irradiations and surfactants.

Acknowledgements

B.A. Bhanvase acknowledges the funding given by the Board of College and University Development (BCUD), University of Pune (grant number BCUD/OSD/184/2009) and Indian Academy of Sciences, Bangalore for providing summer research fellowship in 2009 at the Institute of Chemical Technology, Mumbai. B.A. Bhanvase and S.H. Sonawane are also thankful to Vishwakarma Institute of Technology, Pune for providing the facility for this work.

References

[1] S.S. Ray, M. Okamoto, Polymer/layered silicate nanocomposites: a review from preparation to processing, Prog. Polym. Sci. 28 (2003) 1539–1641.
[2] C. Zeng, L.J. Lee, Poly(methyl methacrylate) and polystyrene/clay nanocomposites prepared by in situ polymerization, Macromolecules 34 (2001) 4098–4103.
[3] P. Meneghetti, S. Qutubuddin, Synthesis of poly(methyl methacrylate) nanocomposites via emulsion polymerization using a zwitterionic surfactant, Langmuir 20 (2004) 3424–3430.
[4] P.C. LeBaron, Z. Wang, T.J. Pinnavaia, Polymer-layered silicate nanocomposites: an overview, Appl. Clay Sci. 15 (1999) 11–29.
[5] Y.K. Kim, Y.S. Choi, M.H. Wang, I.J. Chnug, Synthesis of exfoliated PS/Na-MMT nanocomposites via emulsion polymerization, Chem. Mater. 14 (2002) 4990–4995.
[6] J. Lu, X.P. Zhao, A new approach of enhancing the shear stress of electrorheological fluids of montmorillonite nanocomposite by emulsion intercalation of poly-N-methaniline, J. Colloid Interface Sci. 273 (2004) 651–657.
[7] T.J. Pinnavaia, G.W. Beall, Polymer–Clay Nanocomposites, Wiley, New York, 2001.
[8] M. Okamoto, S. Morita, H. Taguchi, Y.H. Kim, T. Kotaka, H. Tateyama, Synthesis and structure of smectic clay/poly(methyl methacrylate) and clay/polystyrene nanocomposites via in situ intercalative polymerization, Polymer 41 (2000) 3887–3890.
[9] L. Morejon, E. Mendizabal, J.A. Delgado, N. Davidenko, F. Lopez-Dellamary, R. Manriquez, M.P. Ginebra, F.J. Gil, J.A. Planell, Synthesis and characterization of poly (methyl methacrylate-styrene) copolymetric beads for bone cements, Lat. Am. Appl. Res. 35 (2005) 175–182.
[10] J.G. Ryu, S.W. Park, H. Kim, J.W. Lee, Power ultrasound effects for in situ compatibilization of polymer–clay nanocomposites, Mater. Sci. Eng. C 24 (2004) 285–288.
[11] Y. Zhong, Z. Zhu, S.Q. Wang, Synthesis and rheological properties of polystyrene/layered silicate nanocomposite, Polymer 46 (2005) 3006–3013.
[12] M. Laus, M. Camerani, M. Lelli, K. Sparnacci, F. Sandrolini, O. Francescangeli, Hybrid nanocomposites based on polystyrene and a reactive organophilic clay, J. Mater. Sci. 33 (1998) 2883–2888.
[13] X. Fu, S. Qutubuddin, Synthesis of polystyrene–clay nanocomposites, Mater. Lett. 42 (2000) 12–15.
[14] X. Fu, S. Qutubuddin, Polymer–clay nanocomposites: exfoliation of organophilic montmorillonite nanolayers in polystyrene, Polymer 42 (2001) 807–813.
[15] H. Li, Y. Yu, Y. Yang, Synthesis of exfoliated polystyrene/montmorillonite nanocomposite by emulsion polymerization using a zwitterion as the clay modifier, Eur. Polym. J. 41 (2005) 2016–2022.
[16] Y.S. Choi, Y.K. Kim, I.J. Chung, Poly(methyl methacrylate-*co*-styrene)/silicate nanocomposites synthesized by multistep emulsion polymerization, Macromol. Res. 11 (2003) 418–424.
[17] A.R. Mahdavian, M. Ashjari, A.B. Makoo, Preparation of poly(styrene–methyl methacrylate)/SiO_2 composite nanoparticles via emulsion polymerization. An investigation into the compatiblization, Eur. Polym. J. 43 (2007) 336–344.
[18] Z. Matusinovic, M. Rogosic, J. Sipusic, Synthesis and characterization of poly(styrene-co-methyl methacrylate)/layered double hydroxide nanocomposites via in situ polymerization, Polym. Degrad. Stab. 94 (2009) 95–101.
[19] M. Xu, Y.S. Choi, Y.K. Kim, K.H.Wang, I.J. Chung, Synthesis and characterization of exfoliated poly(styrene-co-methyl methacrylate)/clay nanocomposites via emulsion polymerization with AMPS, Polymer 44 (2003) 6387–6395.
[20] G. Diaconu, M. Paulis, J.R. Leiza, Towards the synthesis of high solids content waterborne poly(methyl methacrylate-co-butyl acrylate)/montmorillonite nanocomposites, Polymer 49 (2008) 2444–2454.
[21] R.P. Moraes, A.M. Santos, P.C. Oliveira, F.C.T. Souza, M.D. Amaral, T.S. Valera, N.R. Demarquette, Poly(styrene-co-butyl acrylate)–Brazilian montmorillonite nanocomposites, synthesis of hybrid latexes via miniemulsion polymerization, Macromol. Symp. 245 (2007) 106–115.
[22] L.J. Borthakur, D. Das, S.K. Dolui, Development of core–shell nano composite of poly (styrene-co-methyl acrylate) and bentonite clay by ultra sonic assisted mini-emulsion polymerization, Mater. Chem. Phys. 124 (2010) 1182–1187.
[23] P.R. Gogate, Cavitational reactors for process intensification of chemical processing applications: a critical review, Chem. Eng. Process. 47 (2008) 515–527.
[24] B.M. Teo, S.W. Prescott, M. Ashokkumar, F. Grieser, Ultrasound initiated miniemulsion polymerization of methacrylate monomers, Ultrason. Sonochem. 15 (2008) 89–94.
[25] N. Yin, K. Chen, W. Kang, Preparation of BA/ST/AM nano particles by ultrasonic emulsifier-free emulsion polymerization, Ultrason. Sonochem. 13 (2006) 345–351.
[26] B.M. Teo, M. Ashokkumar, F. Grieser, Microemulsion polymerizations via high-frequency ultrasound irradiation, J. Phys. Chem. B 112 (2008) 5265–5267.
[27] J.G. Ryu, J.W. Lee, Development of poly(methyl methacrylate)–clay nanocomposites by using power ultrasonic wave, Macromol. Res. 10 (2002) 187–193.
[28] T.J. Wooster, M. Golding, P. Sanguansri, Impact of oil type on nanoemulsion formation and Ostwald ripening stability, Langmuir 24 (2008) 12758–12765.
[29] A.J. Webster, M.E. Cates, Stabilization of emulsions by trapped species, Langmuir 14 (1998) 2068–2079.
[30] J. Wang, Y. Hu, S. Wang, Z. Chen, Sonochemical one-directional growth of montmorillonite–polystyrene nanocomposite, Ultrason. Sonochem. 12 (2005) 165–168.
[31] C. Wang, Q. Wang, X. Chen, Intercalated PS/Na^+-MMT nanocomposites prepared by ultrasonically initiated in situ emulsion polymerization, Macromol. Mater. Eng. 290 (2005) 920–926.
[32] L.D. Garciai, O. Picazo, J.C. Merino, J.M. Pastor, Polypropylene–clay nanocomposites: effect of compatibilizing agents on clay dispersion, Eur. Polym. J. 39 (2002) 945–950.
[33] Q. Sun, Y. Deng, Z.L. Wang, Synthesis and characterization of polystyrene–encapsulated laponite composites via miniemulsion polymerization, Macromol. Mater. Eng. 289 (2004) 288–295.
[34] K. Landfester, Synthesis of colloidal particles in miniemulsions, Annu. Rev. Mater. Res. 36 (2006) 231–279.
[35] Y. Cao, Y. Zheng, G. Pan, Radical generation process studies of the cationic surfactants in ultrasonically irradiated emulsion polymerization, Ultrason. Sonochem. 15 (2008) 320–325.
[36] K. Zhang, B.-J. Park, F.-F. Fang, H.J. Choi, Sonochemical preparation of polymer nanocomposites: review, Molecules 14 (2009) 2095–2110.
[37] A. Ganguly, A.K. Bhowmick, Sulfonated styrene-(ethylene-co-butylene)-styrene/montmorillonite clay nanocomposites: synthesis, morphology, and properties, Nanoscale Res. Lett. 3 (2008) 36–44.
[38] W.V. Smith, R.H. Ewart, Kinetics of emulsion polymerization, J. Chem. Phys. 16 (1948) 592–599.
[39] O. Yilmaz, C.N. Cheaburu, D. Durraccio, G. Gulumser, C. Vasile, Preparation of stable acrylate/montmorillonite nanocomposite latex via in situ batch emulsion polymerization: effect of clay types, Appl. Clay Sci. 49 (2010) 288–297.
[40] J.W. Gilman, Flammability and thermal stability studies of polymer layered–silicate (clay) nanocomposites, Appl. Clay Sci. 15 (1999) 31–49.
[41] A. Leszczynska, J. Njuguna, K. Pielichowski, J.R. Banerjee, Polymer/montmorillonite nanocomposites with improved thermal properties. Part I. Factors influencing thermal stability and mechanisms of thermal stability improvement, Thermochim. Acta 453 (2007) 75–96.
[42] P. Maiti, P.H. Nam, M. Okamoto, T. Kotaka, N. Gasegawa, A. Usuki, Influence of crystallization on intercalation, morphology, and mechanical properties of polypropylene/clay nanocomposites, Macromolecules 35 (2002) 2042–2049.
[43] K. Kuraoka, J. Ueno, Preparation of clay/poly(methyl methacrylate) organic–inorganic hybrid gas barrier films via photopolymerization, J. Ceram. Soc. Jpn. 117 (2009) 1243–1245.